JOURNAL OF SOLID STATE CHEMISTRY **122,** 166–175 (1996)
ARTICLE NO. 0098

Nonstoichiometric Zinc Oxide and Indium-Doped Zinc Oxide: Electrical Conductivity and ^{111}In-TDPAC Studies

Ruiping Wang and Arthur W. Sleight[1]

Department of Chemistry, Oregon State University, Corvallis, Oregon 97331-4003

and

Roland Platzer and John A. Gardner

Department of Physics, Oregon State University, Corvallis, Oregon 97331-6507

Received August 8, 1995; accepted December 6, 1995

Indium-doped zinc oxide powders have been prepared which show room-temperature electrical conductivities as high as 30 Ω^{-1} cm^{-1}. The indium doping apparently occurs as $Zn_{1-x}In_xO$, $Zn_{1-y}In_yO_{1+y/2}$, or a combination of these. Optimum conductivity occurs for $Zn_{1-x}In_xO$ where the maximum value of x obtained was about 0.5 at%. This substitution results in a lattice volume expansion of 0.4%. The degrees of sample reduction were determined by iodimetric titration. Time differential perturbed angular correlation (TDPAC) spectroscopy on indium doped zinc oxide is consistent with indium substituting at normal zinc sites in the ZnO lattice. TDPAC studies on zinc oxide annealed under zinc vapors show a second environment for the ^{111}In probe. In this case, there is an unusually high temperature dependence of the electric field gradient which may be caused by a nearby zinc interstitial. An important conclusion of this work is that zinc interstitials are not ionized and do not therefore contribute significantly to the increased conductivity of reduced zinc oxide. © 1996 Academic Press, Inc.

INTRODUCTION

Zinc oxide based materials have many interesting and useful properties. Applications of such materials are especially attractive because of the low cost and lack of toxicity of zinc. Zinc oxide can be heavily n-doped while retaining a very low optical absorption in the visible range. In addition to its many other uses, zinc oxide can be used, therefore, as a transparent conductor in antistatic applications, as window coatings, in solar cell designs, and in flat panel displays. We have prepared highly conductive and transparent zinc oxide powders (1) as well as thin films (2) by appropriate doping. Bulk transport properties of doped zinc oxide have been extensively studied (3–6) since the 1950s. Studies of In-doped single crystal have been reported by Rupprecht (7). Despite these extensive studies, the dominant defect mechanisms in zinc oxide are not completely understood. Here, we report our electrical and ^{111}In-TDPAC (time differential perturbed angular correlation) studies of undoped, Zn-rich and In-doped zinc oxide powders.

The details of the TDPAC technique have been described elsewhere (8). We used the radioactive isotope ^{111}In as TDPAC probe atoms, which are introduced in very small amounts (10^{-9}/formula). Thus, the effect of the radioactive dopants on bulk properties of samples can be neglected. The ^{111}In nucleus has a half-life of 2.8 days and decays by electron capture to an excited state of ^{111}Cd, which then decays to its ground state by successive emission of 171- and 245-keV γ rays through an intermediate state having half-life of 85 ns. If the nucleus is unperturbed by magnetic or electric fields, there is a substantial angular anisotropy between the emission directions of the two γ-rays. The angular anisotropy depends on the time between the two γ-ray emissions if the nucleus is subject to a magnetic field interacting with the Cd nuclear magnetic moment or an electric field gradient (efg) interacting with the nuclear quadrupole moment. Measurement of this time-dependent perturbation is the object of a TDPAC experiment. Only the perturbation due to the first few neighbor shells can be detected by the probe nucleus. Thus, TDPAC provides information about the local environment of the probe. It is a powerful tool to distinguish different defect configurations near probe atoms (9).

Zinc oxide has a hexagonal wurtzite structure in which the oxygen ions are in a hexagonal close packed array, and the zinc ions occupy half of the tetrahedral interstitial positions and have the same relative arrangement as the oxygen ions. The environment of each ion does not have

[1] To whom all correspondence should be addressed.

0022-4596/96 $18.00
Copyright © 1996 by Academic Press, Inc.
All rights of reproduction in any form reserved.

exact tetrahedral symmetry. Instead, the spacing between nearest neighbors along the *c* axis direction is somewhat larger than for the other three neighbors. When a probe ^{111}In atom occupies a substitutional Zn site, it experiences a small axially symmetric efg. If there are other defects around the nuclear probe, different efg's will be measured and the axial symmetry may be destroyed.

EXPERIMENTAL

Zinc-rich zinc oxide powders were prepared by mixing various ratios of Zn powder (5N, Johnson Matthey) and zinc oxide powder (5N, Johnson Matthey). These mixtures were thoroughly ground using an agate mortar and pestle before sealing in silica tubes, which were evacuated to ~50–100 mTorr. The sealed samples were heated at 1200°C for 10 hr with heating and cooling rates of 300°C/hr. The tubes were heated in a slight temperature gradient with the sample placed at the hotter end. Thus, any zinc not incorporated into the oxide phase condensed at the cooler end of the tube, well separated from the oxide. For the TDPAC experiment, the resulting Zn-rich zinc oxide powder is further mixed, in alcohol, with the probe isotope ^{111}In which was purchased from the New England Nuclear Division of Dupont as a HCl solution. The mixture was dried under a heat lamp and then calcined at 1100°C for 5 hr after it was sealed in an evacuated silica tube. Undoped ZnO samples used in the TDPAC experiment were prepared by mixing ZnO powder directly with the ^{111}In isotope in alcohol, and then heating in air or a sealed silica tube at 1100°C for 5 hr.

Preparation of In-doped zinc oxide samples was similar to Zn-rich zinc oxide samples except that various amounts of indium powder were used in the initial synthesis instead of Zn powder. In some cases, In_2O_3 was also added to the reactant mixture in order to increase the oxygen pressure during synthesis. The synthesis temperature was 1000 or 1200°C.

The X-ray diffraction data and unit cell dimension refinements were obtained using a Siemens D-5000 diffractometer and its analysis program. All data were measured at 25°C using a silicon internal standard. Electron Micro-Probe Analysis (EMPA) was used to determine the actual dopant concentration in In-doped ZnO powder. In EMPA analysis, 5 to 15 points were probed. The average is used as the measured value, and the standard deviation is the error shown for that data point. The solubility of the dopant was determined from these data. Scanning electron microscopy (SEM) was used to determine the morphology and particle size of different doped ZnO powders. The conductivities of In-doped zinc oxide powders were measured using the resistivity probe of the LakeShore AC Susceptometer, Model 7000. Because the samples were in powder form, measured conductivities were affected by the powder density and contacts between grains. Thus, the conductivities were measured at various applied pressures. Details of the measuring cell are given elsewhere (1). The measuring contacts were gold plated to achieve low contact resistance; the short circuit resistance was ~0.0003 Ω. Typical samples were ~2 g with a thickness of ~3–5 mm and a density in the range 75–90% of theoretical. The samples used in the conductivity measurements were not ground after synthesis. The measured conductivities generally decreased slightly if the samples were ground. The conductivities of the powders also decreased slightly if they were removed from the cell and then measured a second time. These results suggest that conductivity is somewhat degraded when sintered agglomerates are broken up. The break up of the agglomerates, which is significant especially in Zn-rich ZnO where particle sizes are large, was confirmed by SEM. All conductivity measurements were made at room temperature and a frequency of 5Hz unless otherwise indicated. For the temperature dependence measurements, the four terminal technique was used on pellets which had been sintered at 1200°C for 10 hr in sealed silica tubes.

Iodimetric titrations have been used to determine the amount of excess Zn in Zn-rich ZnO (10–12). The reactions involved are:

(i) triiodide is reduced by active electrons, $I_3^- + 2e^- \rightarrow 3I^-$;

(ii) unreacted triiodide is back titrated with sodium thiosulfate.

From the amount of triiodide used, the number of electrons consumed can be calculated. This method was also used to assess the actual degree of reduction related to doping. Volumetric standards (Aldrich) of 0.1 *N* iodine and 0.1 *N* sodium thiosulfate were used. Zinc oxide powder (~1 g) was dissolved in 5 *N* sulfuric acid with 4 ml of the iodine standard in a capped flask to prevent the evaporation of iodine. The titration solution was stirred with a Teflon coated magnetic bar, and the titration was performed with a 10 ml microburet and a 4 ml volumetric pipette. Dissolving the powder followed by titration consumed about 5 to 10 min. The starch indicator and KI were added close to the end point to achieve maximum sensitivity. The detection limit is estimated to be 0.002 at% excess Zn or 0.004 at% electron in 1g ZnO.

RESULTS

Well oxidized zinc oxide powder is white at room temperature. With a Zn-to-ZnO reactant ratio in the silica tube of 0.001 to 0.004, the color of the reduced powder becomes light blue. This color can be bleached to white if the samples are heated in air above 900°C. The blue color is directly related to the presence of conduction electrons. Thus, higher conductivities were observed for the samples

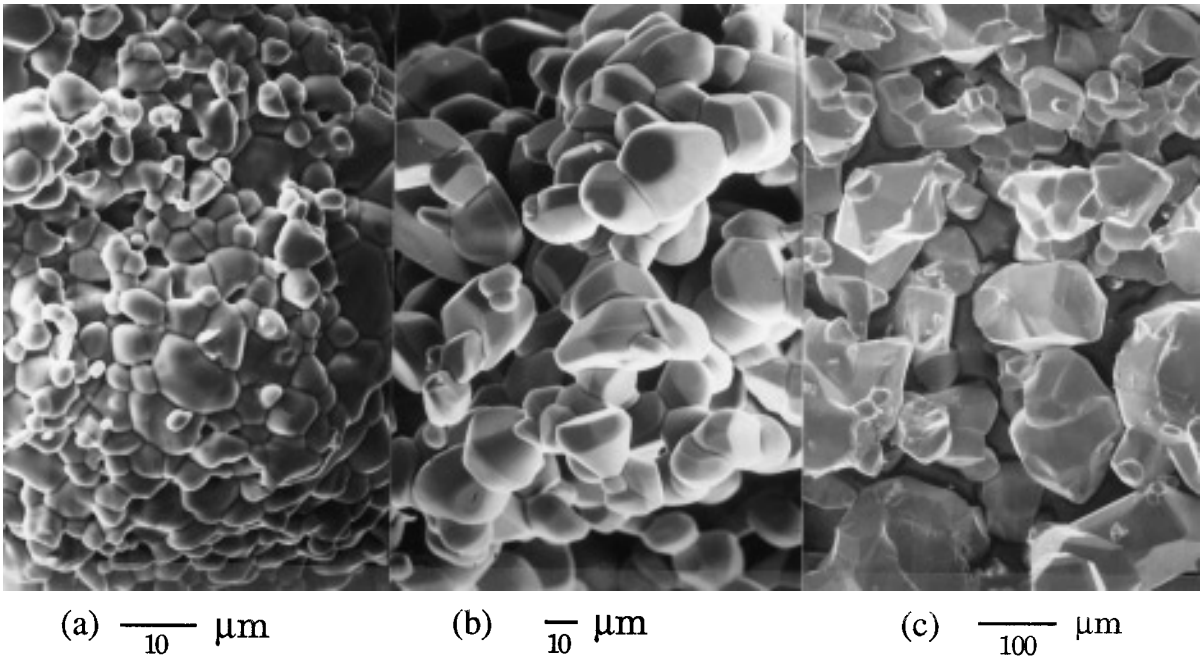

FIG. 1. Electron micrographs of ZnO powder heated at 1200°C for 10 hr (a) in air, (b) in a sealed silica tube, and (c) in a sealed silica tube with Zn and ZnO in a 1/100 ratio.

with a blue color. For a Zn-to-ZnO atomic reactant ratio of greater than 0.004, the color of the Zn-rich zinc oxide powder first becomes green, but this quickly turns to yellow with increasing Zn. The green color can be attributed to a mixture of blue and yellow. The yellow color deepens as the Zn-to-ZnO reactant ratio is increased to 0.007 and does not change for larger ratios, indicating that zinc oxide has become saturated with Zn under these conditions. This is supported by our analytical data in that our samples do not show a change in titratable electrons when prepared with a higher Zn-to-ZnO reactant ratio. The Zn-rich zinc oxide powder has a larger particle size (~80 μm) than that of undoped zinc oxide (~20 μm) heated under the same conditions in an evacuated sealed silica tube. Undoped ZnO heated in air has an even smaller particle size (~5 μm) (Fig. 1). There is, therefore, a regular increase in particle size as zinc oxide is heated under increasing reducing conditions. The particles are approximately equilateral. X-ray lattice parameter refinements for all Zn-rich zinc oxide powders showed $a = 3.2498(2)$ and $c = 5.2065(3)$ Å, regardless of the color or conductivity. Iodimetric titrations showed the electron concentration to be ~0.1 at% for blue zinc oxide and ~0.06 at% for yellow zinc oxide (Fig. 2). Surprisingly, the apparent degree of reduction decreases as the reaction conditions become more reducing. If we assume the titratable electrons in yellow zinc oxide derive from two electrons per excess Zn, the maximum amount of excess Zn in yellow zinc oxide powder can be represented as $Zn_{1.0003}O$. This result is inconsistent with Ehret and Greestone's estimate (13) of 0.02% excess Zn in a red zinc oxide crystal. (A red zinc oxide crystal, when ground, produces a yellow powder.) We observed in a sample of Zn-to-ZnO prepared with a reactant ratio of 0.003, where the color changes from blue to yellow, that the powder next to the silica tube was blue whereas the powder in the center part of the tube was yellow. This strongly suggests that that higher conductivity in blue zinc oxide derives from Si contamination due to the use of a silica tube in synthesis. Silicon is known to act as an electron donor in zinc oxide (14). Microprobe analysis showed Si contamination in these samples. The actual amount of Si cannot be accurately determined due to the calibration limit, but it

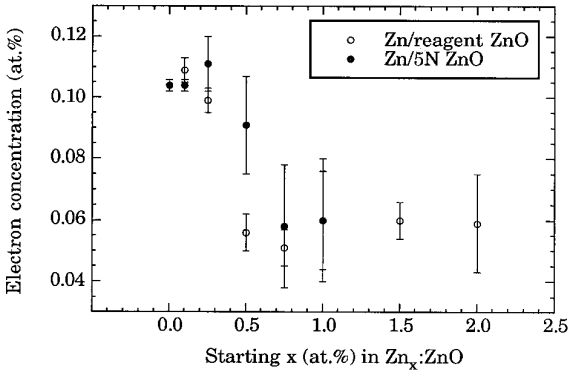

FIG. 2. Electron concentration obtained from iodimetric titration at various starting metal Zn-to-ZnO ratios.

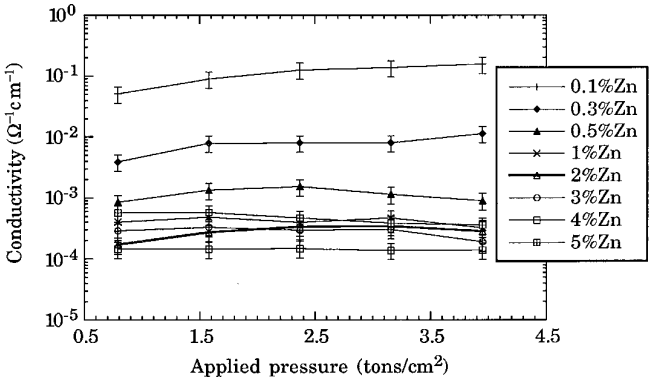

FIG. 3. The conductivity of Zn-rich ZnO powder under applied pressures.

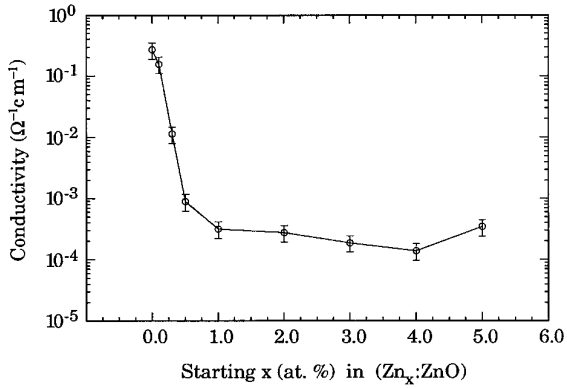

FIG. 4. The conductivity of Zn-rich ZnO prepared using various Zn metal-to-ZnO ratios.

is less than 0.04 at%. Iodimetric titration suggests the maximum contamination is 0.05 at%, assuming Si ionized to +4 in titration. (Contamination with Si is inevitable when using silica containers at high temperature; however, other containers considered cause even more severe problems and cannot be as conveniently sealed or used at high temperatures.) The conductivity of Zn-rich zinc oxide powders changes very little with applied pressure (Fig. 3). It may increase slightly which can be due to some densification and improved contact between grains. The drop in conductivity with increasing pressure sometimes found for samples with larger grains is likely caused by some break up of agglomerates. The conductivity measured at a pressure of 4 ton/cm^2 shows a dramatic decrease in conductivity for the yellow powder relative to the blue powder (Fig. 4). However, this change is still less dramatic than the increase in conductivity which occurs on heating undoped zinc oxide under vacuum or in a sealed tube with very small amounts of elemental zinc.

Doping zinc oxide with indium under reducing conditions causes a dark blue color to develop, which turns to light green if the sample is heated in air at about 900°C for a few hours. However, the optical absorption of the blue materials is so low in the visible region of the spectrum that they are useful as so-called transparent conductors. All products appeared single phase by X-ray diffraction.

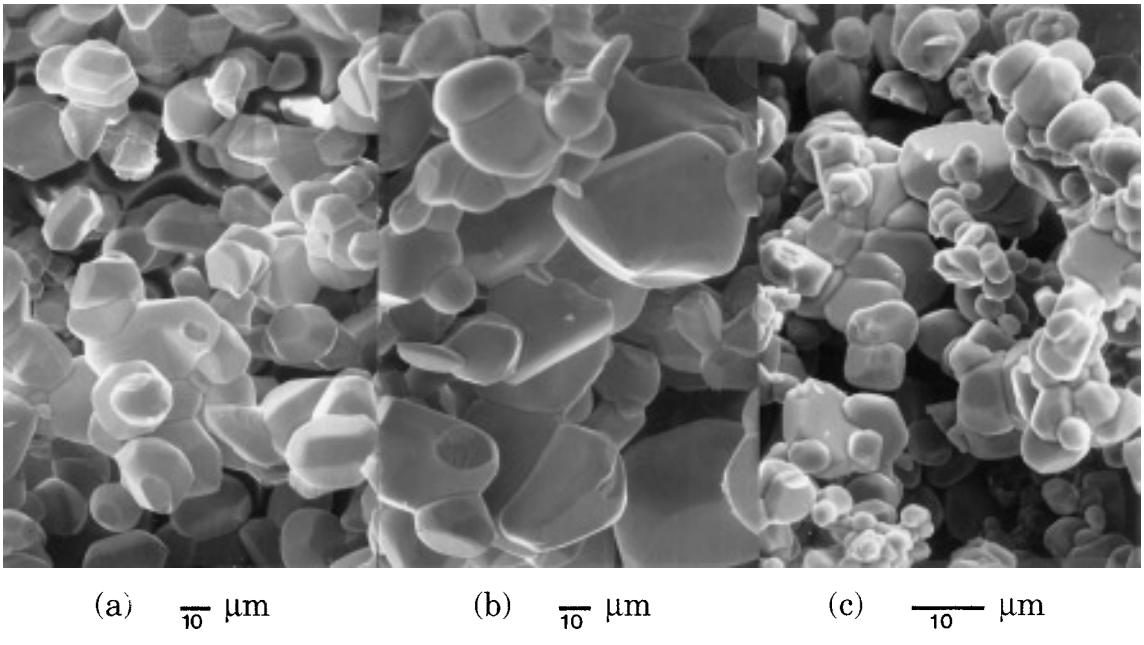

FIG. 5. Electron micrographs of (a) 0.1 at% (1200°C synthesis), (b) 0.5 at% (1200°C synthesis), and (c) 1 at% (1000°C synthesis) In-doped ZnO powder prepared in sealed silica tubes. The percentages are the starting In-to-ZnO mixing ratios.

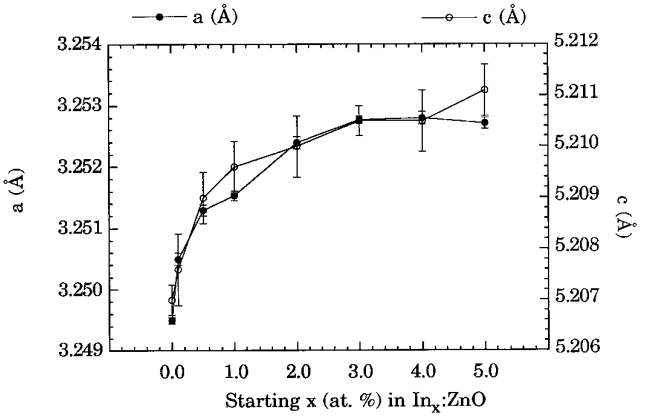

FIG. 6. The lattice constants *a* and *c* at various In metal-to-ZnO ratios.

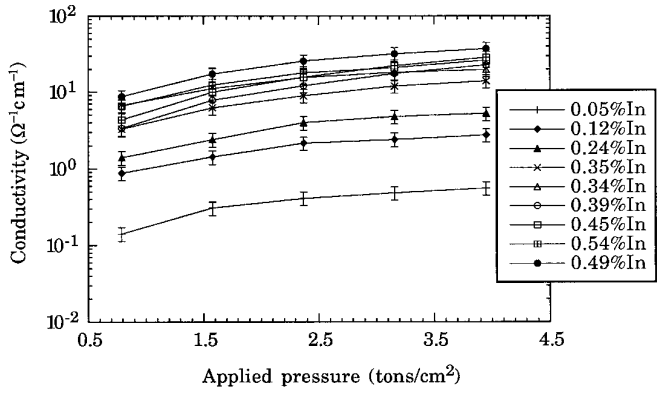

FIG. 8. The conductivity of In-doped ZnO powder at various applied pressures. The labeled In percentages are the true In-doping levels.

SEM showed that higher In-doping levels and higher synthesis temperatures resulted in larger particle sizes (Fig. 5). Figure 6 shows the increase in both *a* and *c* cell dimensions as the amount of indium in zinc oxide increased. Microprobe analysis indicated that the maximum amount of indium present in these samples was about 0.45 at%, and Hall data (2), as well as iodimetric titrations, showed essentially one electron per dopant atom for samples prepared at both 1000 and 1200°C (Fig. 7).

Samples of particular reactant compositions prepared at 1000 and 1200°C gave essentially the same compositions and unit cell dimensions. The conductivities of indium-doped zinc oxide samples synthesized at 1200°C are shown in Fig. 8 as a function of applied pressure. The measured conductivity increased with applied pressure (or the density of the powder). The values obtained at 4 ton/cm^2 are used in Fig. 9 show that the conductivity increases with increasing indium content for samples prepared from zinc oxide and indium metal only. The difference in conductivity for samples synthesized at 1200 or 1000°C is attributed primarily to different particle sizes. Smaller particles have more contacts per unit volume which adds resistivity for the powder sample. The highest conductivity observed is about ~30 Ω^{-1} cm^{-1}. Assuming one free carrier per dopant atom and using the observed conductivities, the apparent mobilities were estimated in the range from 0.1 to 1 cm^2/Vs, which is about 10 times smaller than that of In-doped ZnO thin films (2). The temperature dependence of the conductivity of our indium doped ZnO samples was very small. The variation over the temperature range from 77 to 500 K was less than 10% for all samples. Temperature independent conductivity has also been observed in a single crystal (7) and thin films (2) of In-doped zinc oxide.

The effect of oxygen content on the conductivity of In-doped zinc oxide powder was also examined. The starting amount of indium was fixed at 2 at%, but different ratios of In-to-In_2O_3 were employed. This in effect results in a different partial pressure of oxygen during synthesis. Figure 10 shows the conductivity of samples synthesized at 1000 and 1200°C. The conductivity decreases as the indium

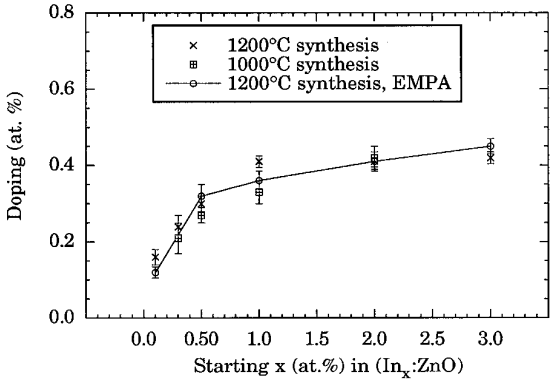

FIG. 7. Electron concentration obtained by iodimetric titrations and In doping level analyzed by EMPA as a function of percentage In metal reactant.

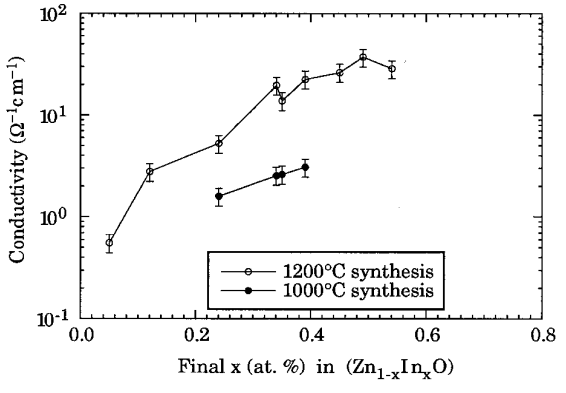

FIG. 9. The conductivity of In-doped ZnO powders at different In-doping levels.

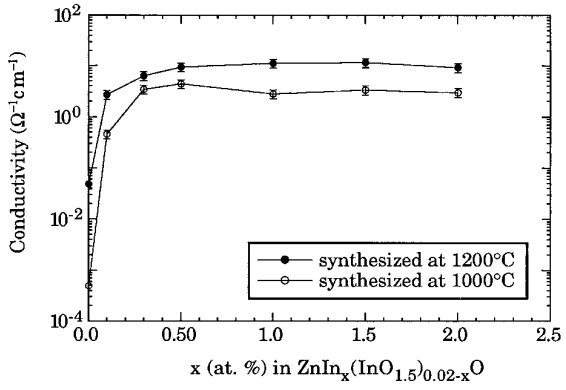

FIG. 10. The conductivity of 2 at% In_x:ZnO at different oxygen contents. The x is the starting In to ZnO mixing ratios.

metal reactant was replaced with In_2O_3. The results of iodimetric titrations confirm the expected lower electron doping when In metal is replaced with indium oxide in the reactant mixture (Fig. 11).

Two samples of undoped and two of indium doped zinc oxide were studied by TDPAC. The atomic In-to-ZnO reactant ratios for the two In-doped samples were 0.003 and 0.01, and EMPA showed actual indium concentrations of 0.25 and 0.36 at%, respectively, for these two samples. The TDPAC spectra of undoped (white) zinc oxide, slightly reduced undoped zinc oxide (light blue), and the 0.25 and 0.36 at% In-doped zinc oxides (both blue) showed that all indium atoms were in the same environment. This site is subject to a modest efg having axial symmetry (site A). Site$A$ has $\nu_{QA} = 31.4(2)$ MHz and $\eta = 0.00(2)$ at room temperature. Figure 12 shows the TDPAC time spectrum $A_2G_2(t)$ of an undoped zinc oxide sample (a) and the Fourier Transform (FT) of the undoped and 0.36 at% In-doped zinc oxide samples (b). The indium-doped zinc oxide spectra showed broader peak widths than that of the undoped zinc oxide. We assume that this site is indium substituted

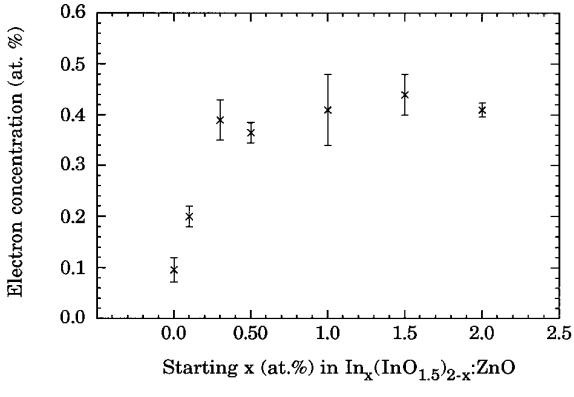

FIG. 11. The iodimetric titration results of the 2 at% In-mixed ZnO samples synthesized at 1200°C with different oxygen contents.

for Zn on a normal Zn site. The TDPAC frequency ν_{QA} for site A was independent of temperature from room temperature up to about 200°C, then increased at higher temperatures (Fig. 13). This temperature dependence has been attributed to an increased concentration of conduction electrons (15). The temperature dependence of the ν_{QA} can be fit to

$$\nu_{QA}(T) = \nu_{QA}(0)(1 + \alpha \exp(-E_f/kT)),$$

where $\nu_{QA}(0) = 31.4(2)$ MHz, $\alpha = 1.2(1)$, and $E_f = 0.4(1)$ eV. The value of E_f from the fit is the same as that reported by Wolf *et al.* (16).

The spectra for the two samples richest in Zn, yellow and orange zinc oxide, showed that indium atoms occupy a second site (site B) in addition to site A. Figure 14 shows the TDPAC time spectrum (a) and its FT (b) for a yellow zinc oxide sample. The B site has a slightly asymmetric efg with $\nu_{QB} = 170(2)$ MHz and $\eta = 0.12(2)$ at room temperature. Witthuhn *et al.* (17) interpreted this site as a site with a Zn interstitial next to the probe atom. It was proposed that the interstitial Zn occupies position 2 in Fig. 15. The efg of this site, which is proportional to ν_{QB}, decreases as the temperature increases. This type of temperature dependence has been observed in many metals and semiconductors (18–21). The temperature dependence of this site follows $T^{3/2}$ behavior, which is generally attributed to excitation of resonant modes in the local phonon density of states. The temperature dependence (Fig. 16) of the ν_{QB} can be fit to

$$\nu_{QB}(T) = \nu_{QB}(0)(1 - BT^{3/2}),$$

where $\nu_{QB}(0) = 174(2)$ MHz and $B = 4.0 \times 10^{-6}(2)$. Only zinc oxide powder prepared with more than 0.4 at% excess Zn showed the B site, and a larger fraction of the site B was observed when a greater excess of Zn was used during synthesis. The occupation probability of site B increased with increasing excess Zn, but the fraction of ^{111}In probe at the B site never exceeded 1/3 that of the A site.

DISCUSSION

Doping of zinc oxide powders with indium results in high electrical conductivity (30 Ω^{-1} cm^{-1}) at room temperature, but even higher conductivity was obtained from an In-doped single crystal (7) (200 Ω^{-1} cm^{-1}), from In-doped thin films (2) (1100 Ω^{-1} cm^{-1}), and from gallium-doped zinc oxide powders (1) (300 Ω^{-1} cm^{-1}). However, for In-doped zinc oxide thin films and Ga-doped zinc oxide powders much higher doping levels were obtained. The conductivities of Ga-doped and In-doped zinc oxide powders are, in fact, comparable at the 0.5% doping level.

Various mechanisms for indium incorporation into the

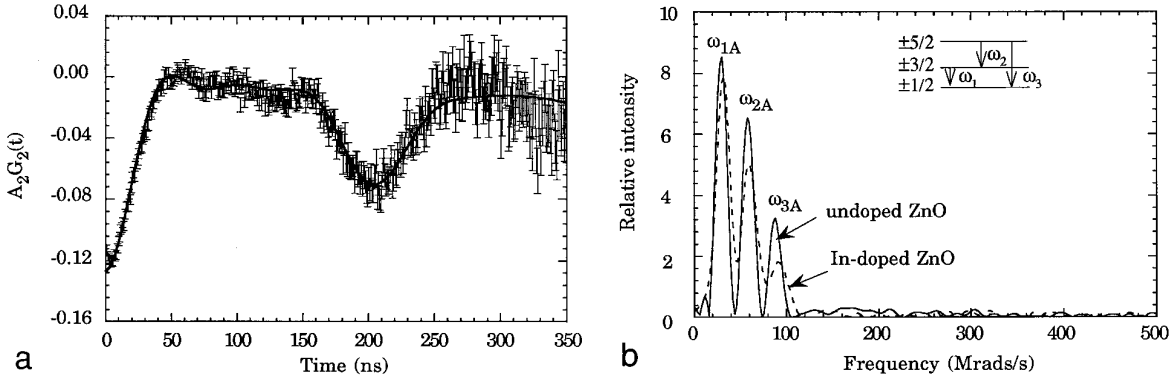

FIG. 12. TDPAC time spectrum (a) and its FT (b) of the site *A*. The solid line in (a) is the fitted curve.

zinc oxide lattice can be proposed. An indium interstitial mechanism ($ZnIn_xO$) would give one electron per indium if indium is ionized to In^{1+} and three electrons per indium if indium is ionized to In^{3+}. However, both mechanisms can be excluded by our iodimetric titrations, assuming that iodine will oxidize In^{1+} to In^{3+}. Hall data on thin films of In-doped zinc oxide never show more than one free carrier per dopant atom (2), again denying the possibility of interstitial indium ionized to In^{3+}. A formulation consistent with our results is $Zn_{1-x}In_xO$. Assuming that indium is ionized to In^{3+}, one free carrier per indium results.

Increasing the oxygen partial pressure during synthesis of indium-doped zinc oxide causes a decrease in conductivity (Fig. 10) and a decrease in the degree of reduction as determined by iodimetric titrations (Fig. 11). In the case of Ga-doped zinc oxide, the solubility of Ga increased from 2.7 to at least 4 at% with increased oxygen content (1). However, only a slight increase in indium solubility in zinc oxide occurred with increased oxygen pressure during synthesis. The lower solubility of indium in zinc oxide at all oxygen contents is presumably due to the larger size of In^{3+} relative to Zn^{2+} and Ga^{3+}.

Analysis of TDPAC data indicates that at least some of the ^{111}In probe atoms are always on a site with axial symmetry which we designate as site *A*. This site is presumably a normal Zn lattice site in ZnO. However, the interstitial octahedral and tetrahedral sites also both possess axial symmetry. We cannot rule out indium at one of these interstitial sites based on TDPAC data, but we have ruled out this possibility based on our Hall data and iodimetric titrations. Site *B* is observed only in zinc-rich zinc oxide,

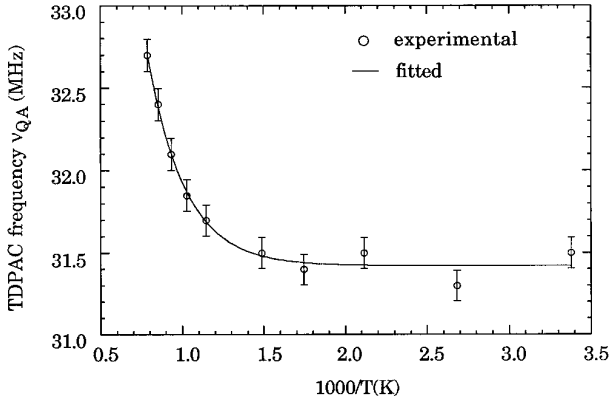

FIG. 13. The temperature dependence of the TDPAC frequency of site *A*.

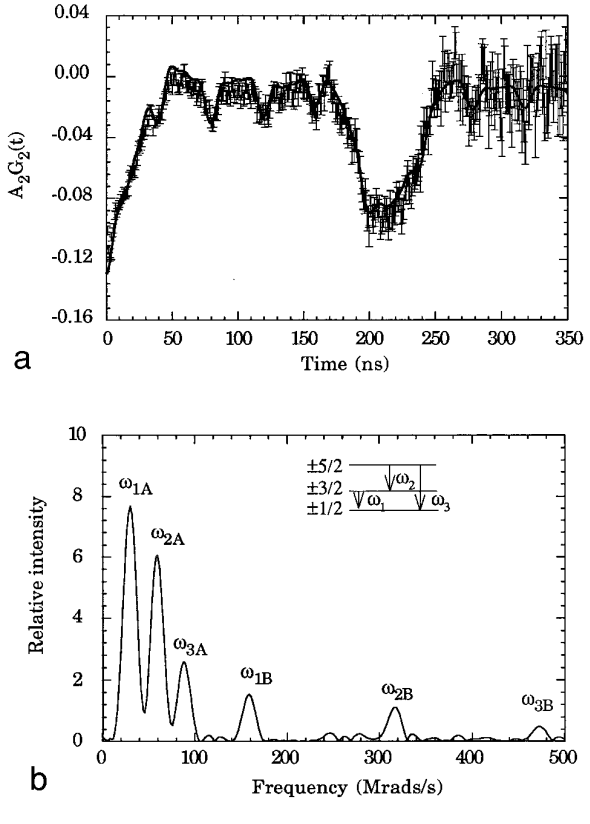

FIG. 14. TDPAC time spectrum (a) and its FT (b) of 1 at% Zn-excess ZnO. Both *A* and *B* sites are labeled.

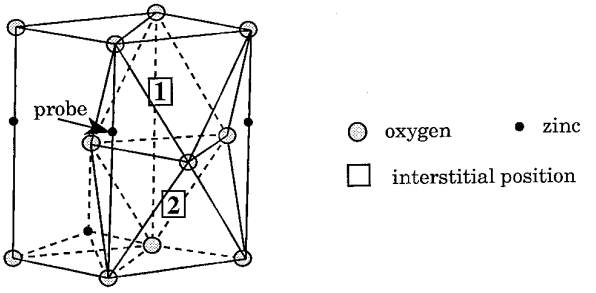

FIG. 15. The schematic of the interstitial Zn.

and it is not axial symmetric. Site *B* cannot be a substitutional Zn lattice site, an interstitial tetrahedral site, or an interstitial octahedral site because all these sites have axial symmetry. A candidate for this site is a substitutional lattice site which is perturbed by the presence of nearby interstitial zinc. Considering the low concentrations of the ^{111}In probe and the interstitial zinc, the TDPAC signal from site *B* would be too weak to be observable unless there is an attraction between the probe and the interstitial zinc. A rationalization of this attraction is given below. Another possibility for site *B* would have the ^{111}In probe at a substitutional Zn lattice site with a nearby oxygen vacancy. This can presumably be ruled out because the two sites are both positive ($In_{Zn}^{\cdot}$ and $V_{\ddot{O}}$) and would therefore repel each other.

The situation for zinc oxide without the intentional addition of a third element is poorly understood. As normally prepared, zinc oxide is white. Heating in evacuated silica tubes causes a light blue color to develop, and the conductivity increases significantly. Using the maximum Si contamination suggested by iodimetric titration (0.05 at%) and the mobility estimated (1) for low Ga or In doping levels (0.1 cm^2/Vs), the calculated conductivity is 0.3 Ω^{-1} cm^{-1}, which is the same as our measured value. (Studies (1, 2) on doped ZnO show that the mobility is more dependent on electron concentration than on the specific dopant.) Therefore, we believe that the color and conductivity of zinc oxide heated in sealed silica tubes is likely related to a low level of unintentional doping by silicon, i.e., $Zn_{1-x}Si_xO$. Others have also suggested (22) that the conductivity in zinc oxide is more likely related to impurities than to the nonstoichiometry of zinc oxide. A serious problem is that only a couple of the several hundred papers on properties of zinc oxide give any information about the purity of their material. In one study where an effort was made to obtain the highest purity zinc oxide, analyses showed no major impurity except Si (23). However, Si is a good electron donor in zinc oxide prepared under reducing conditions and thus will be a very important issue in $Zn_{1+x}O$ samples.

Heating zinc oxide together with sufficient zinc metal in a sealed silica tube results in the development of a yellow-to-red color. The conductivity of this material is higher than that of "undoped" white zinc oxide. However, an observation not previously reported is that this yellow-red zinc oxide is actually less conducting than light blue zinc oxide which is presumably closer to the one-to-one stoichiometry. Most workers believe that the dominant defect present in zinc oxide annealed under elemental zinc vapors is a zinc interstitial. Many conclude that this zinc interstitial is completely ionized to Zn^{2+}, but others have concluded that this interstitial has a charge of plus one (3, 24). We suggest the formation of $(Zn_2)^{2+}$ dimers when zinc oxide is annealed under zinc vapors. These would then be analogous to the better known $(Hg_2)^{2+}$ and $(Cd_2)^{2+}$ dimers. In fact, such a $(Zn_2)^{2+}$ species has been postulated to be responsible for the red color that develops when molten $ZnCl_2$ is annealed under vapors of elemental zinc (25). Such a $(Zn_2)^{2+}$ species could form if a zinc atom is placed at an interstitial site:

$$Zn^{2+}O + xZn^0 \rightarrow Zn^{2+}(Zn_i^0)_xO \rightarrow Zn_{1-x}^{2+}(Zn_2^{1+})_xO.$$

Conceptually, the neutral interstitial zinc atom forms a bond to Zn^{2+} at a normal lattice site. After bond formation, both zincs in the cluster are formally Zn^{1+}. Thus, relative to the neutral lattice, the zinc of the cluster which sits on a normal zinc lattice site has become negative (Zn_{Zn}'), and the zinc at the interstitial site has become positive ($Zn_{Zn}^{\cdot}$). Although the $(Zn_2)^{2+}$ cluster does not normally have a dipole moment, it develops one when it is imbedded in the zinc oxide lattice. There will, therefore, be an attraction between the positive charged ^{111}In probe site and the negative end of the dipole in the $(Zn_2)^{2+}$ cluster, that is, an attraction between positive $In_{Zn}^{\cdot}$ and negative Zn_{Zn}'. This attraction is, however, induced by the nearby presence of interstitial zinc which is mobile enough at high temperatures to find the highly dilute ^{111}In probe. In this model, the presence of interstitial zinc ($Zn_{1+x}O$) would not

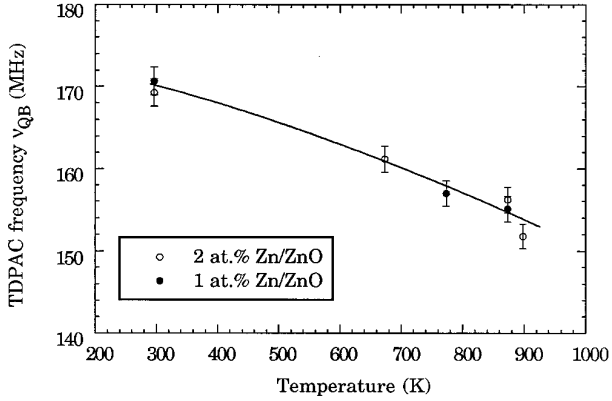

FIG. 16. The temperature dependence of the TDPAC frequency of site *B*.

increase or decrease the number of free electron carriers with increasing x because the extra electrons have been trapped in a Zn–Zn bond. These electrons are sufficiently high in energy to be available for the iodimetric titration, but they do not contribute significantly to conductivity. However, this defect would increase scattering of conduction electrons and thus be one factor decreasing mobility, and therefore conductivity, as its concentration increases. It is also reasonable to suggest that the presence of the $(Zn_2)^{2+}$ clusters in the zinc oxide lattice cause a decrease in the solubility of Si in zinc oxide. The decreased Si content would then be the primary factor causing the reduced conductivity as the excess zinc in the zinc oxide lattice is increased. Further studies are underway to test this hypothesis.

The remaining question is the position of interstitial Zn in the zinc oxide lattice. There is both an octahedral and tetrahedral site to consider. Placing the interstitial Zn in the tetrahedral site would result in a well defined $(Zn_2)^{2+}$ cluster with the cluster axis aligned along the c axis of the zinc oxide lattice. One problem with this approach is that it would result in an unreasonably short Zn–Zn distance of 1.5 Å. One possibility is that lattice relaxation will produce a more favorable Zn–Zn distance. On the other hand, there is more than enough room for Zn^{2+} in the octahedral site of the zinc oxide lattice. The Zn–O distance would be 2.28 Å whereas the Zn–O bond length from the sum of ionic radii is 2.12 Å. A Zn^{2+} ion rattling in this site might explain the large temperature dependence of the site B efg from TDPAC measurements, but according to our cluster model, zinc is formally Zn^{1+} not Zn^{2+}. This univalent cation will be larger, and rattling in the octahedron of oxygens is not assured. Alternately, we may consider Zn in an interstitial site formed by six Zn^{2+} cations. This site is displaced by 0.6 Å along the z axis relative to the center of the octahedral site formed by oxygens. In this view, we consider the Zn–Zn distance to be 2.28 Å if the interstitial Zn is at the center of the octahedron formed by Zn atoms. Such a distance is not unreasonable in a $(Zn_2)^{2+}$ cluster considering that the Hg–Hg distance in the $(Hg_2)^{2+}$ cluster ranges from 2.9 to 2.4 Å (26). However, for interstitial Zn centered in an octahedron of Zn atoms, there are six Zn–Zn distances of 2.28 Å, three Zn–O distances of 2.0, and three Zn–O distances of 2.7. The TDPAC data suggest an abnormal thermal vibration for Zn at this site. Such displacements might be expected if a binuclear cluster is energetically preferred. A Raman band at about 175 cm^{-1} has been reported (24) for $(Zn_2)^{2+}$ clusters in $ZnCl_2$. We searched for such a band in Zn-rich zinc oxide powders and single crystals. Although a weak band near 175 cm^{-1} may be present in such Zn-rich materials, further studies would be required for confirmation and interpretation.

Most previous workers have assumed that the Zn interstitials of zinc-rich zinc oxide are ionized, and they have no explanation for the yellow-red color which develops in such materials. We believe, on the other hand, that the 4s electrons of zinc are trapped in a metal bonded cluster. This leads to a state in the band gap but close to the valence band. Excitation from this state to the conduction band is then a natural explanation of the yellow-red color. Because this state is occupied by a pair of electrons, there is no EPR signal associated with this defect.

Nonstoichiometric zinc oxide is frequently used as a textbook example of an oxide where the predominant defect is a metal interstitial. Because of the observation of increased electrical conductivity when zinc oxide is reduced, the conclusion has been that the zinc interstitials have ionized and donated electrons to the conduction band. We reject that conclusion. We believe that the yellow-to-red color of $Zn_{1+x}O$ is directly associated with interstitial zinc but this interstitial zinc is not ionized. Instead, metal–metal bonded clusters form which trap the electrons in metal–metal bonds. This defect does not increase conductivity in any substantial way. Evidence for this view has existed before, but has not been fully appreciated. For example, Thomas noted that certain annealing treatments of $Zn_{1+x}O$ could destroy the conductivity but the yellow-to-red color persisted (3).

We believe that the conductivity that develops on treatment of zinc oxide under reducing conditions is due to impurities. Even if reactants are essentially free of impurities, the impurities are easily introduced during synthesis, processing, or crystal growth. Common containers such as SiO_2 and Al_2O_3 serve as good sources of the excellent electron donors Si^{4+} and Al^{3+}. These impurities are not evident before a reducing treatment. This is because the impurities are compensated by extra oxygen ($Zn_{1-x}Si_xO_{1+x}$), and a white insulator results. Under mildly reducing conditions, the extra oxygen is removed. Then, $Zn_{1-x}Si_xO_{1+x}$ becomes $Zn_{1-x}Si_xO$, which is blue and conducting. The effect on conductivity is dramatic due to the high mobility of these electrons. On more severe reduction, zinc interstitials and the yellow-to-red color develops.

The highest value of x in $Zn_{1+x}O$ that we achieved was about 0.0003, a value very similar to those of many other studies. One other study, however, gave a much higher value of x. This was an X-ray diffraction study examining electron density at interstitial sites. The conclusion was an x value of 0.015 (27). That study has recently been repeated; the result is consistent with an x value of 0.0003 in red single crystals of $Zn_{1+x}O$ (28).

ACKNOWLEDGMENTS

This work was supported by E.I. du Pont de Nemours and Co., the U.S. Department of Energy, and a Deutscheforschungsgemeindshaft fellowship for R. Platzer.

REFERENCES

1. R. P. Wang and A. W. Sleight, *Chem. Mater.*, in press.
2. R. P. Wang, L. L. H. King, and A. W. Sleight, submitted for publication.
3. D. G. Thomas, *J. Phys. Chem. Solids* **3,** 229 (1957).
4. K. Haufle and A. L. Vierk, *Z. Physik. Chem.* (*Leipzig*) **196,** 160 (1950).
5. E. E. Hahn, *J. Appl. Phys.* **22,** 855 (1951).
6. K. Haufle and J. Bloock, *Z. Physik.* (*Leipzig*) **196,** 438 (1951).
7. H. Rupprecht, *J. Phys. Chem. Solids* **6,** 144 (1958).
8. H. Frauenfelder and R. M. Steffen, *in* ''Alpha-, Beta-, and Gamma-Ray Spectroscopy'' (K. Siegbahn, Ed.), p. 997. North-Holland, Amsterdam, 1965.
9. R. P. Wang, J. A. Gardner, W. E. Evenson, and J. A. Sommers, *Phys. Rev. B* **47,** 638 (1993).
10. W. J. Moore and E. Secco, *J. Chem. Phys.* **26,** 942 (1957).
11. W. J. Moore, *J. Chem. Phys.* **53,** 845 (1956).
12. J. Deren and E. Fryt, *Chem. Anal.* **8,** 365 (1963).
13. Ehret and Greenstone, *J. Am. Chem. Soc.* **65,** 872 (1943).
14. T. Minami, H. Sato, H. Nanto, and S. Takata, *Jpn. J. Appl. Phys.* **25,** L776 (1986).
15. H. Wolf, Diplomarbeit, Erlangen, unpublished, 1985.
16. H. Wolf, S. Deubler, D. Forkel, H. Foettinger, M. Iwatschenko-Borho, F. Meyer, M. Renn, W. Witthuhn, and R. Helbig, ''Defects in Semiconductors'' (H. J. von Bardeleben, Ed.), *Materials Science Forum* **10–12,** 863 (1986).
17. S. Deubler, J. Meier, R. Schütz, and W. Witthuhn, *Nucl. Inst. Meth. Phys. Res. B* **63,** 223 (1992).
18. R. Keitel, W. Engel, H. Föttinger, K. Forkel, M. Iwtschenko-Borho, F. Meyer, and W. Witthuhn, *Hyperfine Interactions* **15/16,** 425 (1983).
19. W. Engel, W. Klinger, and W. Witthuhn, *Hyperfine Interactions* **9,** 247 (1981).
20. K. Nishiyama, F. Dimmling, T. Kornrumpf, and D. Riegel, *Phys. Rev. Lett.* **37,** 357 (1976).
21. P. Heubes, *et al.*, *in* ''Proceedings of the International Conference on Hyperfine Interactions Studied in Nuclear Reactions and Decay, Uppsala, Sweden, 1974'' (E. Karlsson and R. Wäppling, Ed.), p. 208. Univ. of Uppsala, Uppsala, Sweden, 1974; P. Heubes, dissertation, Universität Erlangen, 1975.
22. C. Gonzalez, D. Block, R. T. Cox, and A. Hervé, *J. Crystal Growth* **59,** 357 (1982).
23. K. I. Hagemark and L. C. Chacka, *J. Solid State Chem.* **15,** 261–270 (1975).
24. E. Secco and W. Moore, *J. Chem. Phys.* **26,** 942 (1957).
25. D. H. Kerridge and S. A. Tariq, *J. Chem. Soc.* (*A*), 1122 (1967).
26. John D. Corbett, *Inorg. Chem.* **1,** 700 (1962).
27. G. P. Mohanty and L. V. Azároff, *J. Chem. Phys.* **35,** 1268 (1961).
28. H. Sawada, R. Wang, and A. W. Sleight, *J. Solid State Chem.*, in press.